



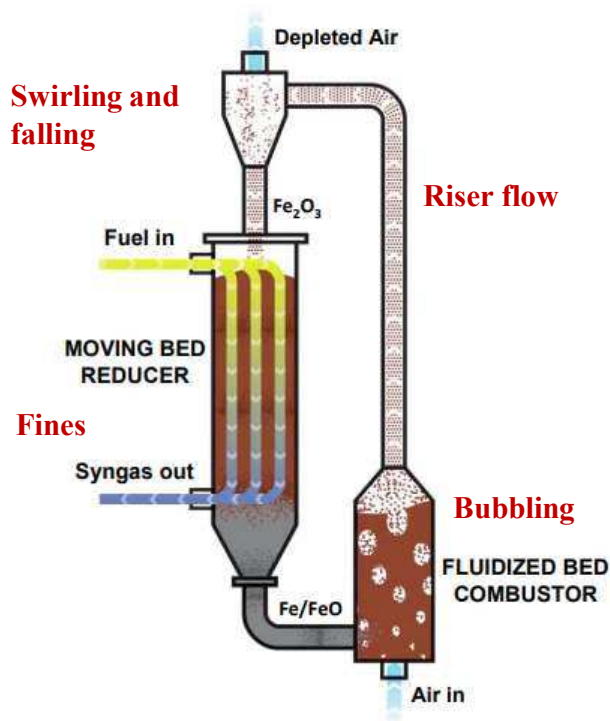
THE OHIO STATE UNIVERSITY

**MACHINE LEARNING-BASED FORCE MODEL FOR
IRREGULAR-SHAPED PARTICLES IN GAS-SOLID FLOWS**

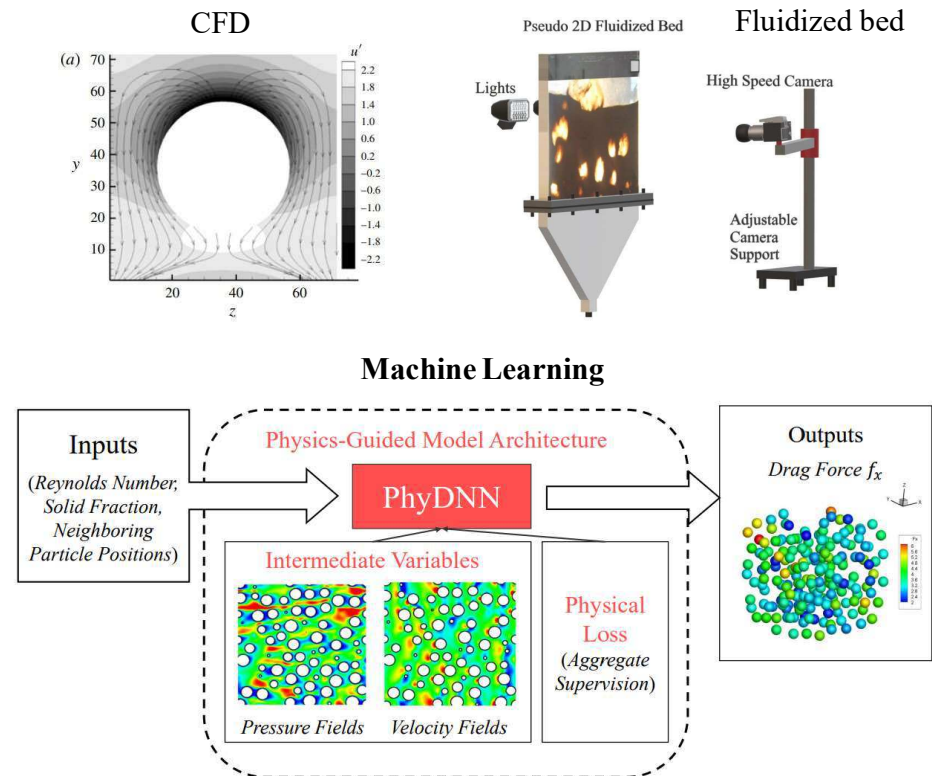
SooHwan Hwang, Liang-Shih Fan



Gas-Solid Flows



Interaction Forces



Qiang Zhou et al., *Journal of Fluid Mechanics*, 765 (2015)
 Cesar Martin Venier et al. *International Journal of Numerical Methods for Heat and Fluid Flow* (2019)
 Long He et al., *Powder Technology* 345 (2019)

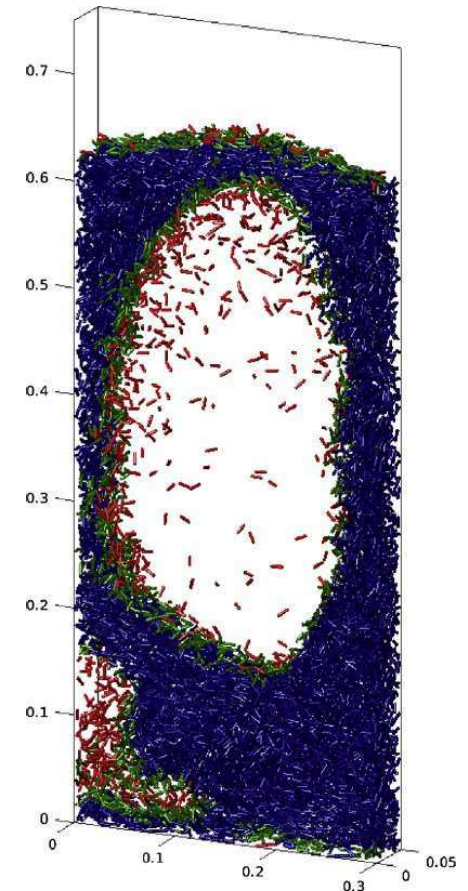
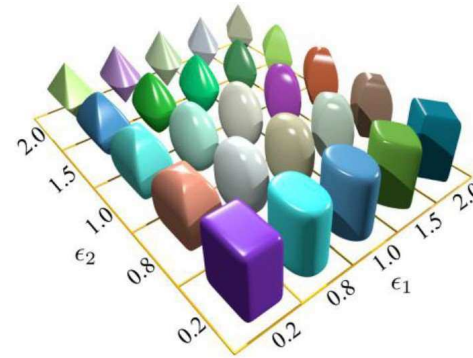


Non-spherical particle

- Difficult to define the geometrical factors sphericity, flatness, elongation and circularity, etc.
- Data for the interaction force between non-spherical particles and the fluids are limited.
- Correlation may be highly-nonlinear.

Objectives

- Developing a neural network-based force model for a diversity of non-spherical particles.



Shiwei Zhao et al., Int J Numer Anal Methods Geomech., 43 (2019)

Vinay V. Mahajan et al., Chemical Engineering Science, 192 (2018)



Spherical Harmonic (SH)

$$\nabla^2 f = \frac{1}{r^2} \frac{\partial}{\partial r} \left(r^2 \frac{\partial f}{\partial r} \right) + \frac{1}{r^2 \sin \theta} \frac{\partial}{\partial \theta} \left(\sin \theta \frac{\partial f}{\partial \theta} \right) + \frac{1}{r^2 \sin^2 \theta} \frac{\partial^2 f}{\partial \varphi^2} = 0.$$

$$f(r, \theta, \varphi) = \sum_{\ell=0}^{\infty} \sum_{m=-\ell}^{\ell} f_{\ell}^m r^{\ell} Y_{\ell}^m(\theta, \varphi).$$

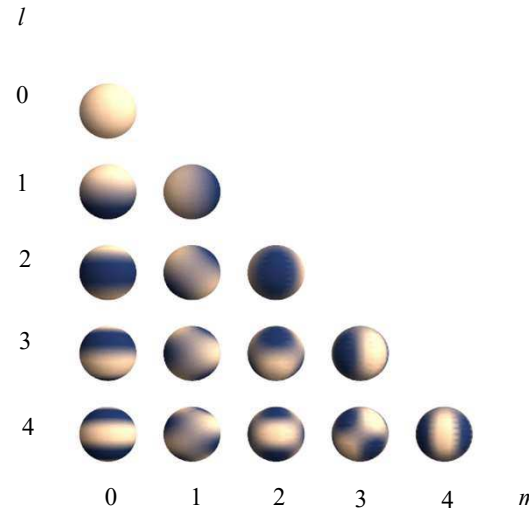
$$X = (x, y, z) = \sum_{l=1}^8 \sum_{m=-l}^l C_l^m Y_l^m(\varphi_1, \varphi_2)$$

$$C_l = \begin{pmatrix} C_{x,l}^{-l} & \dots & C_{x,l}^0 & \dots & C_{x,l}^l \\ C_{y,l}^{-l} & \dots & C_{y,l}^0 & \dots & C_{y,l}^l \\ C_{z,l}^{-l} & \dots & C_{z,l}^0 & \dots & C_{z,l}^l \end{pmatrix}$$

$$= \begin{pmatrix} k_{x,l}(\alpha_{x,2l} - \alpha_{x,2l+1}i) & \dots & k_{x,l}\alpha_{x,1} & \dots & k_{x,l}(\alpha_{x,2l} + \alpha_{x,2l+1}i) \\ k_{y,l}(\alpha_{y,2l} - \alpha_{y,2l+1}i) & \dots & k_{y,l}\alpha_{y,1} & \dots & k_{y,l}(\alpha_{y,2l} + \alpha_{y,2l+1}i) \\ k_{z,l}(\alpha_{z,2l} - \alpha_{z,2l+1}i) & \dots & k_{z,l}\alpha_{z,1} & \dots & k_{z,l}(\alpha_{z,2l} + \alpha_{z,2l+1}i) \end{pmatrix}$$

$$k_{i,l} = \sqrt{\frac{d_{i,l}^2}{\alpha_{1,1}^2 + 2 \sum_{j=2}^{2l+1} \alpha_{i,j}^2}}, \quad i \in (x, y, z)$$

$$d_{i,l} = \frac{d \sqrt{\frac{\pi}{3}(1+EI^2+EI^2FI^2)}}{\sum_{k=2}^8 \binom{2}{k}^{1.387}} \binom{2}{l}^{1.387}$$



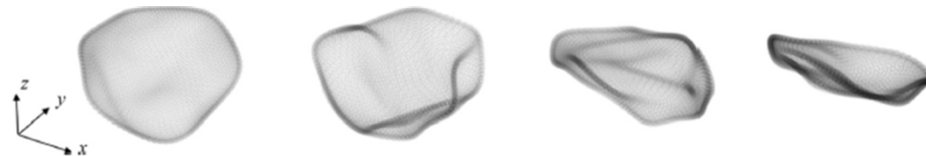
Combine linearly,
Higher weight on higher $l \rightarrow$ high d
 $d \sim$ roughness

$d/EI/FI = 0.25/1/1$

$0.5/1/1$

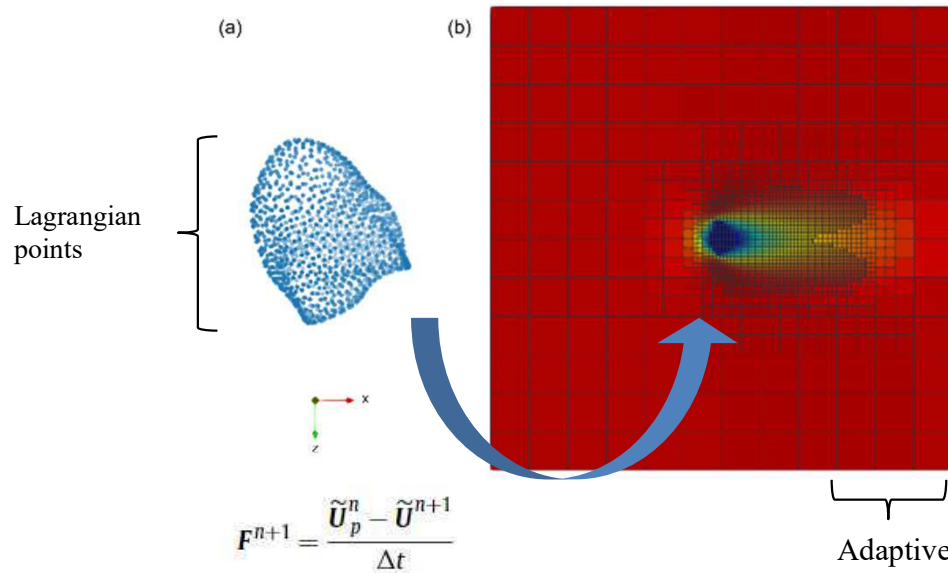
$0.5/0.5/1$

$0.5/0.25/1$





Particle-Resolved Direct Numerical Simulation (PR-DNS)



$$\mathbf{F}^{n+1} = \frac{\tilde{\mathbf{U}}_p^n - \tilde{\mathbf{U}}^{n+1}}{\Delta t}$$

Direct forcing scheme
 $\tilde{\mathbf{U}}_p^n = 0$ for fixed particles

Adaptive mesh refinement based on:

$$\Omega = \frac{b}{a+b}$$

$$a = \text{trace}(\mathbf{A}^T \mathbf{A}) = \sum_{i=1}^3 \sum_{j=1}^3 (\mathbf{A}_{ij})^2,$$

$$b = \text{trace}(\mathbf{B}^T \mathbf{B}) = \sum_{i=1}^3 \sum_{j=1}^3 (\mathbf{B}_{ij})^2.$$

$$\frac{\partial f}{\partial t} + \mathbf{v} \cdot \nabla f = \frac{g-f}{\tau}$$

$$f(0, t) \approx g(0, t) + \frac{\tau}{\delta t} (g(-v\delta t, t - \delta t) + g(0, t))$$

$$\mathbf{F} = \int f(0, t) v_x \Xi d\mathbf{v}, \quad \Xi = \begin{pmatrix} 1 \\ \mathbf{v} \end{pmatrix}$$

$$\frac{\partial \mathbf{W}}{\partial t} + \nabla \cdot \mathbf{F} = 0, \quad \mathbf{W} = \begin{pmatrix} \rho \\ \rho \mathbf{u} \end{pmatrix}$$

$$g = \begin{cases} \frac{\rho}{4\pi}, & \text{if } (\mathbf{u} - \mathbf{v})^2 = c^2 \\ 0, & \text{otherwise} \end{cases}$$

Simplified Sphere function for incompressible flows

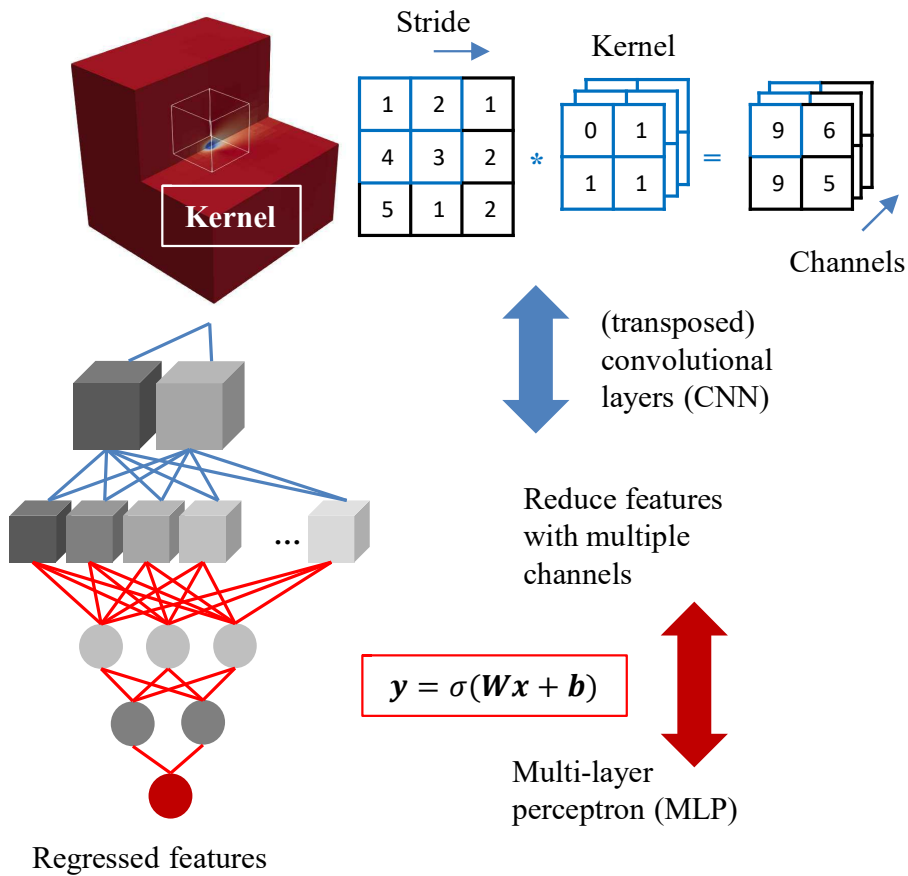
Gas Kinetic Scheme

$$\nabla \mathbf{V} = \frac{1}{2}(\nabla \mathbf{V} + \nabla \mathbf{V}^T) + \frac{1}{2}(\nabla \mathbf{V} - \nabla \mathbf{V}^T)$$

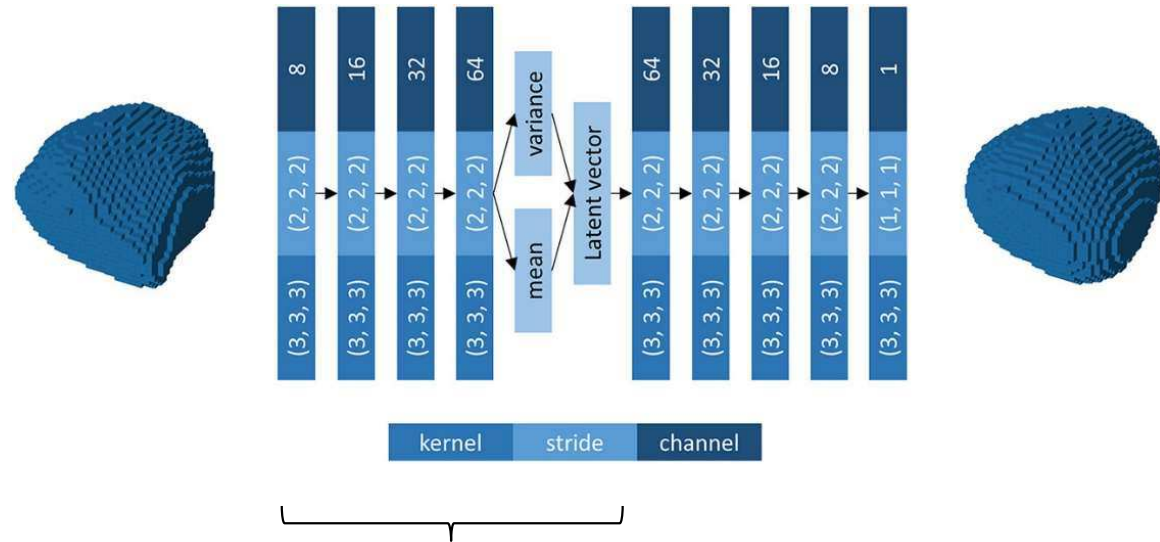
$$= \mathbf{A} + \mathbf{B},$$



Neural Networks



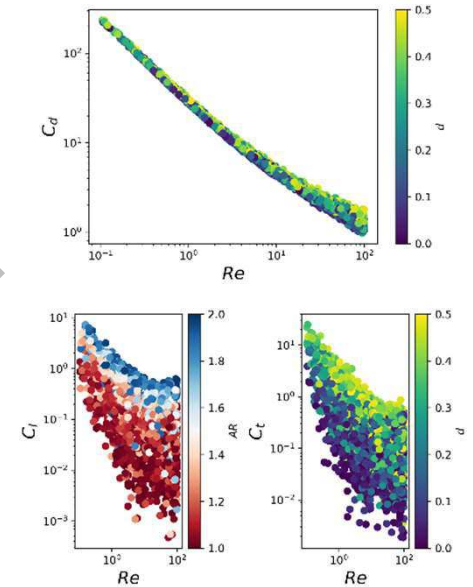
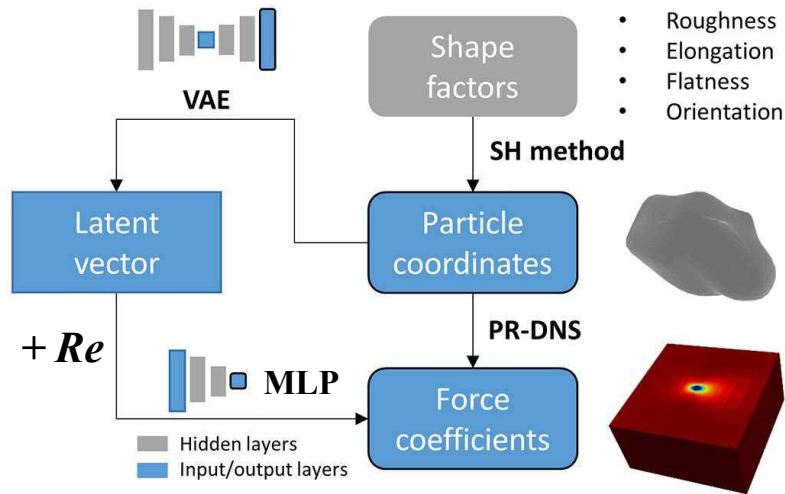
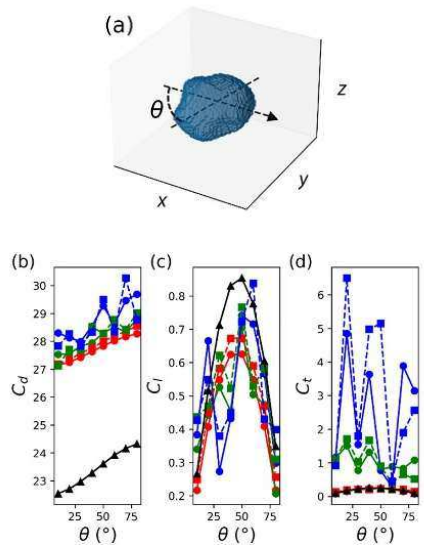
Variational Auto-Encoder (VAE)



- Encoder
 $48^3 \rightarrow 24^3 \times 8 \rightarrow 12^3 \times 16 \rightarrow 6^3 \times 32 \rightarrow 3^3 \times 64 \rightarrow 27$
 - MLP/Regularization
 $27 \rightarrow 128 \times 2 \rightarrow 128$ (**latent**)
- Vertices (Decoder, TCNN)
 Force coefficients (MLP)
 Flow fields (PIEP, TCNN)



Interaction Force Model for Single Particles

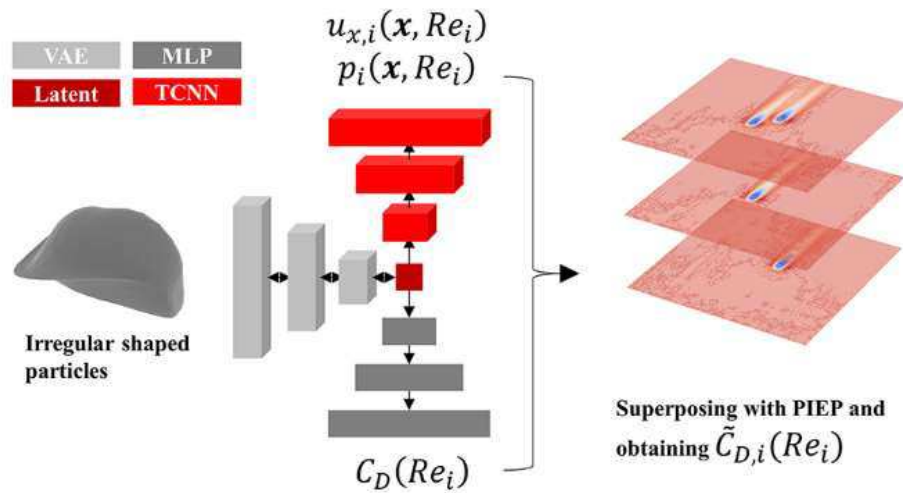


CFD results

MLP results (MSE) C_d : 7.9 (3.3% MAPE)
 C_l : 0.00546
 C_t : 0.0647

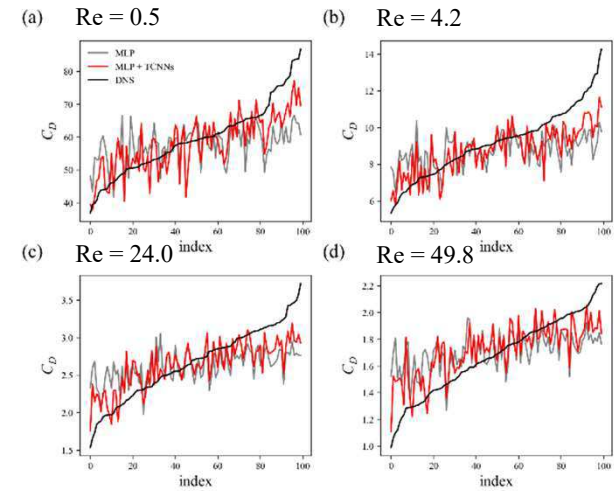
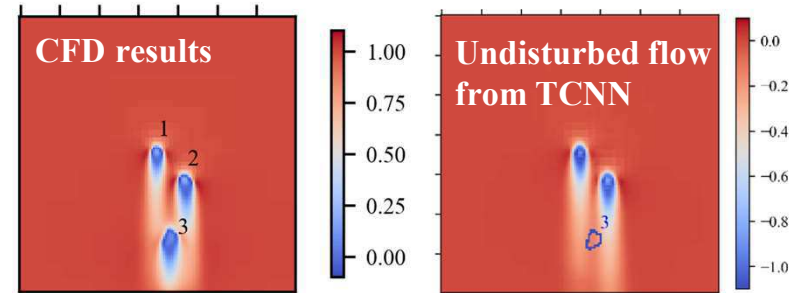


PIEP with MLP and TCNN



$$\tilde{F}_{qs,i} = \bar{F}_{drag}(Re_i, \varphi) + \frac{\rho u_{mac}^2 A}{2} C_{D,i} \left\{ \frac{1}{u_{mac}} \sum_{\substack{j=1 \\ j \neq i}}^N \overline{u_{j \rightarrow i}}^S \right\}$$

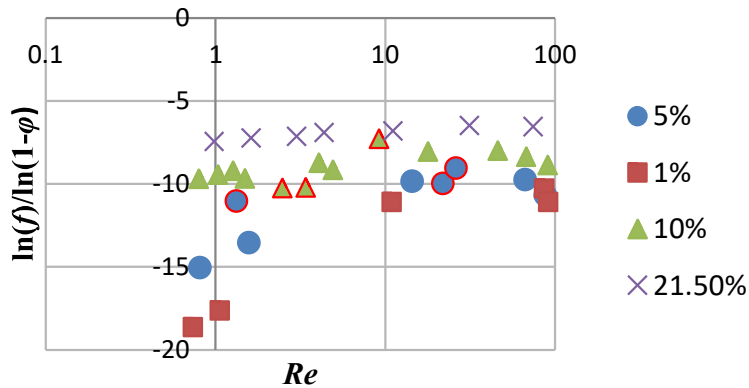
100 different particles with 0.5% ($1 < AR < 2, 0 < d < 0.5$)



PIEP: Pairwise Interaction Extended Point-particle model
Soohwan Hwang et al., *Chemical Engineering Science* 266, 118299 (2023)

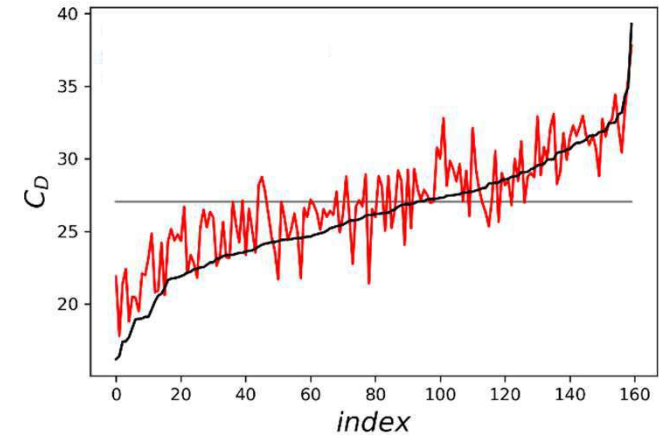
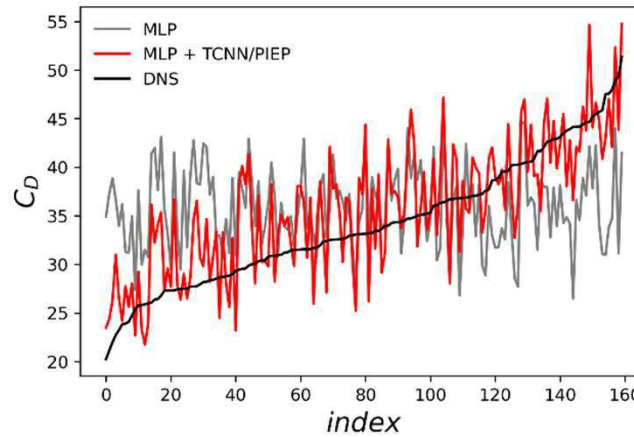


PIEP for dense systems



$Re = 1.8$, polydisperse ($\varphi = 0.06, d = 0 \sim 0.5$)
 MAPE: 12%
 R2 : 0.46

$Re = 2.2$, monodisperse ($\varphi = 0.05, d = 0.49$)
 MAPE: 7%
 R2: 0.70



$$\bar{C}_D(Re_i, \varphi, d) = C_{D,i} \cdot f(Re_i, \varphi, d)$$

$$x = (\ln(Re) - 3.5)^2$$

$$\frac{\log(f)}{\log(1-\varphi)} = a(\varphi)x + b(\varphi)$$

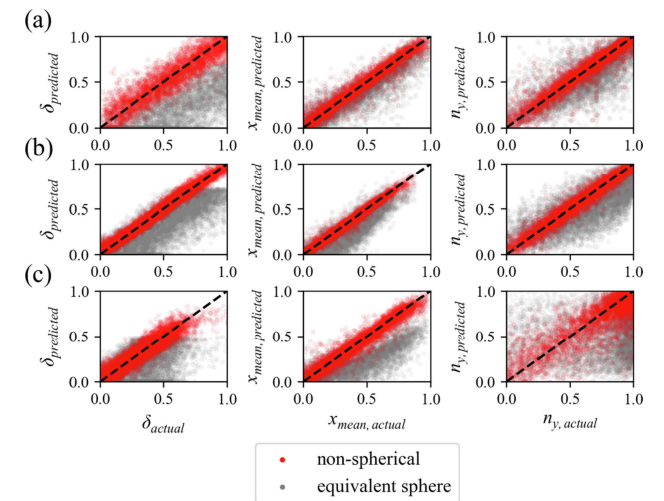
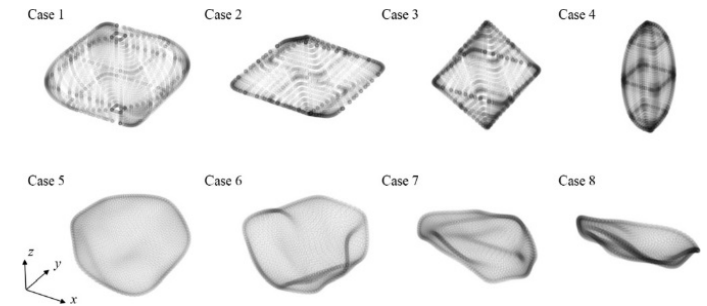
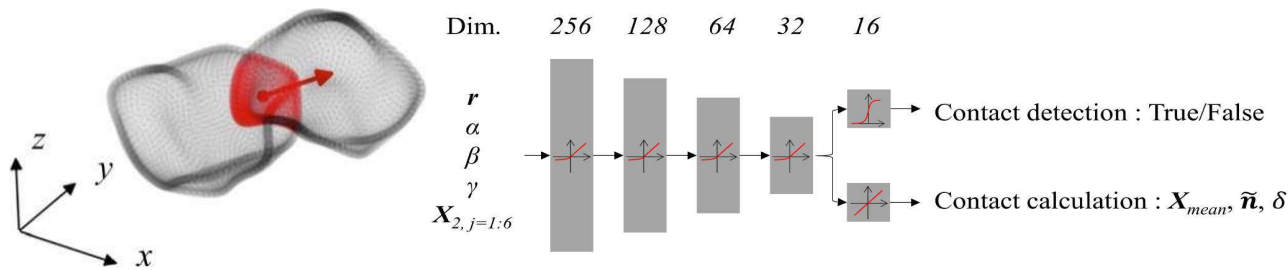
$$a(\varphi) = 0.18 \ln(\varphi) + 0.23$$

$$b(\varphi) = 18.1\varphi - 10.4$$



Contact model

- Develop a ML-based contact model outside of DEM loop to predict contact properties
- Regular, irregular-shaped particles
- Significant improvement of computational efficiency





- This study provides ML-based force models for the irregular particle flows, which is practical in industry.
- The PIEP-based approach is efficient in that it mainly requires data for single particles.
- This study also provides computationally efficient collision force model, which can be applied to CFD-DEM.